Original Article

Development of recombinant canine single-chain insulin analogues, evaluation of their insulin receptor binding capacity and ability to stimulate glucose uptake

Jamie P. Adams [1], Angela L. Holder, Brian Catchpole *

Department of Pathology and Pathogen Biology, Royal Veterinary College, University of London, Hawkshead Lane, Hatfield, Hertfordshire AL9 7TA, UK

* Corresponding author. Tel.: +44 170 766 6388.
E-mail address: bcatchpole@rvc.ac.uk (B. Catchpole).
[1] Current address: Boehringer Ingelheim, Ellesfield Avenue, Bracknell, Berkshire RG12 8YS, UK.

Abstract

Virtually all diabetic dogs require exogenous insulin therapy to control their hyperglycaemia. In the UK, the only licensed insulin product currently available is a purified porcine insulin preparation. Recombinant insulin is somewhat problematic in terms of its manufacture, as the gene product (preproinsulin) undergoes substantial post-translational modification in pancreatic β cells before it becomes biologically active. The aim of the present study was to develop recombinant canine single-chain insulin (SCI) analogues that could be produced in a prokaryotic expression system and which would require minimal processing. Three recombinant SCI constructs were developed in a prokaryotic expression vector, by replacing the insulin C-peptide sequence with one encoding a synthetic peptide (GGGPGKR) or with one of two insulin-like growth factor (IGF)-2 C-peptide coding sequences (human: SRVSRRSR; canine: SRVTRRSSR). Recombinant proteins were expressed in the periplasmic fraction of *E. coli* and assessed for their ability to bind to the insulin and IGF-1 receptors and to stimulate glucose uptake in 3T3-L1 adipocytes.

All three recombinant SCI analogues demonstrated preferential binding to the insulin receptor, compared to the IGF-1 receptor, with increased binding compared to recombinant canine proinsulin. The recombinant SCI analogues stimulated glucose uptake in 3T3-L1 adipocytes compared to negligible uptake using recombinant canine proinsulin, with the canine insulin/cIGF-2 chimaeric SCI analogue demonstrating the greatest effect. Thus, biologically-active recombinant canine SCI analogues can be produced relatively easily in bacteria, which could potentially be used for treatment of diabetic dogs.

Keywords: Insulin; Insulin receptor; Canine diabetes; Glucose uptake

Introduction

Diabetes mellitus in dogs is characterised by the presence of hyperglycaemia caused by an absolute or relative deficiency in the pancreatic β cell hormone, insulin (Catchpole et al., 2008). Virtually all diabetic dogs require administration of exogenous insulin to control their blood glucose concentration. Whereas recombinant insulin is used to treat human diabetic patients, in the UK there is currently only one licensed insulin product available for treatment of diabetes in companion animals, which consists of purified porcine insulin (Caninsulin, MSD Animal Health)[1]. Recombinant human insulin has been used for many years in North America for treatment of canine diabetes, where until recently there was no FDA-approved insulin for companion animals (Rucinsky et al., 2010).

Production of purified beef and pork insulin has been scaled down, with the introduction of recombinant techniques for production of human insulin. Since the supply of bovine and porcine insulin for veterinary use generally relies on human market availability, insulin for diabetic dogs is likely to become increasingly limited. Indeed, in recent years, bovine insulin products (formerly Insuvet soluble, lente and protamine zinc insulin, Zoetis) have been withdrawn from the veterinary market. Thus, there is an anticipated need for development of recombinant canine insulin preparations.

Biologically active insulin is synthesised in pancreatic β cells by extensive post-translational modification of preproinsulin. After folding and disulphide bond formation between insulin A and B chains, cleavage of the connecting C-peptide is required for biological activity (Fig. 1A). Proinsulin demonstrates a somewhat modest 1-2% affinity for binding to the insulin receptor (INSR) compared to insulin and it is thought that there are two main reasons

[1] See: http://www.vmd.defra.gov.uk/productinformationdatabase/SPC_Documents/SPC_124274.doc.

for this (Peavy et al., 1985); insulin C-peptide does not seem to allow enough molecular flexibility to facilitate interaction with INSR binding sites and it interferes with important receptor-binding residues such as glycine at position A1. This presents a challenge for commercial production of recombinant insulin, since most methods are based on use of prokaryotic expression systems, with bacteria and yeast lacking the necessary cellular machinery and enzymes required for correct folding and processing of proinsulin to insulin.

The first recombinant insulin to become commercially available (Humulin, Eli Lilly) was based on a process whereby insulin A and B chains were produced separately in bacteria, then combined to form the biologically active molecule (Riggs and Itakura, 1979). However this process is somewhat inefficient and subsequently different techniques have been employed for commercial production of recombinant human insulin, which usually involves synthesis of a precursor molecule that is subjected to chemical and/or enzymatic modification (Christensen et al., 1991).

An alternative approach to synthesis of recombinant insulin is to produce single chain insulin (SCI) analogues, which do not require post-translational modification to exert their biological activity (Kristensen et al., 1995). In SCI analogues, the proinsulin C-peptide is substituted with alternative linking peptide sequences that allow folding and disulphide bond formation between A and B chains, but which do not require cleavage and interfere with binding to the INSR much less than the native C-peptide. One such construct, developed for gene therapy of diabetes, involved substituting the insulin C-peptide with a synthetic peptide linker (Lee et al., 2000).

There are other members of the insulin superfamily, with the most important being the

insulin-like growth factors IGF-1 and IGF-2 (Chan and Steiner, 2000). Unlike insulin, IGF-1 and IGF-2 do not require cleavage of their C-peptide to bind to their cognate receptors. IGF-2 has been implicated in the syndrome of non-islet cell tumour hypoglycaemia, which involves production of an IGF-2 related peptide by tumour cells that acts on insulin receptors to cause hypoglycaemia (Boari et al., 1995; LeRoith, 2004; Zini et al., 2007). Thus, insulin and IGF-2 both have glucose-lowering properties that might be exploited for developing a novel therapeutic for canine diabetes.

The aim of the present study was to develop canine SCI analogues, whereby the insulin C-peptide was substituted with either a synthetic peptide linker or alternatively the human or canine IGF-2 C-peptide sequence, to express these recombinant SCI analogues in bacteria and to assess their ability to bind to the INSR and stimulate glucose uptake in cultured cells. The hypothesis was that such SCI analogues would be biologically active, without any requirement for post-translational modification.

Materials and methods

Generation of canine single-chain insulin analogue constructs

The coding sequence for recombinant canine proinsulin (rcPROINS) was amplified by PCR with a high-fidelity proof-reading polymerase (Easy-A High-Fidelity PCR cloning kit, Stratagene) using canine insulinoma cDNA as the template. Restriction sites for *Eco*RI and *Sph*I were incorporated into the forward and reverse primers respectively (see Appendix: Supplementary material) to allow for subsequent directional subcloning of rcPROINS from the pSC-A cloning vector (Stratagene) to the pTAC-MAT-Tag-2 expression vector (Sigma-Aldrich).

Three SCI analogues were designed, each substituting the proinsulin C-peptide with a different peptide linker sequence (Fig. 1B). The pSC-A/rcPROINS plasmid DNA was used as the template for further PCR to generate the necessary coding sequences for each of the constructs. Initially, primers designed to anneal to insulin A chain or B chain were modified by adding specific synthetic oligonucleotide sequences encoding the linking GGGPGKR peptide as well as restriction sites to facilitate ligation of the two elements into a single construct. The pTAC-MAT-Tag-2/rcINS[GGGPGKR] construct was completed by digestion of PCR products, followed by ligation into the pTAC-MAT-Tag-2 vector (see Appendix: Supplementary material for more information on cloning strategy).

A synthetic oligonucleotide dimer encoding the FLAG epitope (Asp-Tyr-Lys-Asp-Asp-Asp-Asp-Lys) was inserted into these two expression constructs immediately upstream of and in frame with the proinsulin coding sequence. Subsequently, pTAC-MAT-Tag-2/rcPROINS plasmid DNA was used as the template to generate amplicons required to create the canine insulin/IGF-2 C-peptide chimeric constructs, rcINS[cIGF-2C] and rcINS[hIGF-2C] (see Appendix: Supplementary material for more information on cloning strategy). Constructs were subcloned into the pFLAG-ATS (Sigma-Aldrich) periplasmic expression vector that had been modified to incorporate a 3′ metal affinity tag (pFLAG-MAT-Tag-ATS). Using the same methodology, the MAT sequence was also inserted into the pFLAG-ATS+BAP (bacterial alkaline phosphatase) vector (Sigma-Aldrich) to create pFLAG-MAT-Tag-ATS+BAP, used as a positive control for expression studies. Plasmid DNA was transformed into BL-21(T1) *E. coli* (Sigma-Aldrich) for expression of recombinant proteins.

Expression of recombinant SCI analogues

Expression of recombinant protein was performed in *E. coli*, transformed with plasmid

DNA encoding rcPROINS or the various SCI analogues. An individual colony was inoculated into 10 mL LB broth containing 100 μg/mL ampicillin (LB Liquid Amp, Fermentas) and incubated in an orbital shaker at 145 rpm, 37 °C overnight. Bacterial cultures were diluted by adding 1 mL to 50 mL pre-warmed LB/Amp in a 250 mL baffled shaker flask (Erlenmeyer Culture Flask Baffled Base, BD Falcon) and incubated at 145 rpm, 37 °C until they reached the desired turbidity (optical density at 600 nm; OD_{600} = 2.0), as measured with an Eppendorf BioPhotometer. Isopropyl β-D-1-thiogalactopyranoside (IPTG, Sigma-Aldrich) was added to cultures at 1 mM for 4 h to stimulate recombinant protein expression. Bacterial pellets were obtained by centrifuging samples at 2500 *g* for 15 min. Bacteria were lysed in 10 M guanidium hydrochloride (Sigma-Aldrich) in PBS pH 7.2, centrifuged at 13,000 *g* for 2 min and supernatants used for analysis. Alternatively bacterial pellets from 20 mL culture were resuspended in 40 mL/g osmotic shock buffer (500 mM sucrose, 30 mM Tris-HCl, 1 mM EDTA, pH 8.0; all Sigma-Aldrich) and centrifuged at 3500 *g* at 10 °C for 10 min. Pellets were then resuspended in 25 mL/g ice-cold distilled water, incubated for 5 min, then centrifuged at 3500 *g* for 10 min at 4 °C to obtain the periplasmic fraction.

Analysis of recombinant SCI analogues by ELISA and Western blotting

Fifty microlitres of bacterial lysate were added to nickel-coated ELISA wells (Ni-NTA HisSorb strips, Qiagen) and incubated at room temperature for 2 h. After three washes with 200 μL PBS supplemented with 0.1% Tween-20 (PBST), 50 μL per well of anti-FLAG M2 HRP antibody conjugate (Sigma-Aldrich) diluted 1:10,000 in PBST was added and plates incubated for 1 h. After a further six washes with PBST, binding of anti-FLAG was detected by adding 50 μL per well of 3,3′,5,5′-Tetramethylbenzidine (TMB liquid substrate system for ELISA, Sigma-Aldrich) and the reaction stopped by adding 100 μL 2M sulphuric acid (SLS). The optical density at 450 nm (OD_{450}) of each well was then measured using a SpectraMax M2

169 microplate reader. Results are shown as the mean OD of triplicate wells, following subtraction
170 of values for background wells containing lysis buffer only. Estimation of FLAG-tagged
171 recombinant protein concentration in bacterial periplasmic samples was performed by
172 reference to a standard curve, constructed using a dilution series of FLAG-BAP control protein
173 (Sigma-Aldrich) in an anti-FLAG ELISA.
174
175 Bacterial periplasmic fractions were reduced using 10% β-mercaptoethanol (Sigma-
176 Aldrich) in sodium dodecyl sulphate (SDS) buffer (RunBlue LDS sample buffer, Expedeon)
177 for 15 min at 95 °C. Denatured proteins were separated under reducing conditions using 16%
178 PAGE gels (RunBlue Gel, Expedeon) in an X-cell SureLock Mini-cell (Invitrogen) at constant
179 180V for 60 min. Transfer of the separated proteins to nitrocellulose membranes was performed
180 in the X-cell II Blot module (Invitrogen) using transfer buffer (PAGEgel.com) under reducing
181 conditions at constant 30 V for 60 min. Membranes were rinsed with PBST, blocked in PBST
182 supplemented with 5% dried skimmed milk (Marvel, Premier International Food) overnight,
183 then incubated for 60 min in 15 mL of anti-FLAG HRP antibody diluted 1:5000 in PBST/5%
184 milk. Membranes were subsequently washed four times with PBST and antibody binding
185 detected by enhanced chemiluminescence (Amersham ECL Western Blotting Detection
186 Reagents, GE Healthcare) using autoradiography film (Amersham Hyperfilm ECL, GE
187 Healthcare).
188
189 *Receptor-binding assays*
190 Flat bottomed MaxiSorp microplates (Nunc) were coated with 50 µL per well
191 recombinant human insulin receptor (rhINSR) or IGF-1 receptor (rhIGF-1R) (R&D Systems)
192 at 4 µg/mL and incubated overnight at 4 °C. Negative control wells contained diluent (0.15 M
193 PBS) only. After three washes with PBST, plates were blocked with 100 µL per well PBST

supplemented with 5% bovine serum albumin (BSA), incubated for 3 h and washed a further three times. Recombinant FLAG-tagged SCI analogues from bacterial periplasmic fractions were added at 50 µL per well at the indicated concentrations. Biotinylated bovine insulin (Sigma-Aldrich) or biotinylated recombinant human IGF-1 (bIGF-1; IBT Systems) were used as positive controls. Plates were incubated for 1 h prior to washing three times with PBST, then 100 µL per well of anti-FLAG HRP at 1:10,000 dilution or streptavidin HRP (Sigma-Aldrich) at 1:200 dilution (both in PBST/0.1% BSA) added. Plates were incubated for 1 h, washed six times with PBST then 50 µL per well of supersensitive TMB (Sigma-Aldrich) added. The reaction was stopped by adding 100 µL 2M sulphuric acid and the absorbance at 450 nm (OD_{450}) measured using a SpectraMax M2 microplate reader. Results were calculated as the mean OD_{450} of triplicate wells following subtraction of background values in the absence of receptor; binding curves were constructed and analysed according to a four-parameter logistic equation using GraphPad Prism version 5.0 for Windows. Relative binding activities were compared using one-way ANOVA, followed by the Student's *t*-test with the Bonferroni post-hoc correction applied (PASW Statistics for Windows). Adjusted values were considered significant at $P < 0.05$.

Glucose uptake assay

The ability of recombinant SCI analogues to induce a biological effect was assessed by measuring insulin-stimulated glucose uptake in cultured adipocytes. This was achieved using a mouse fibroblast cell line (3T3-L1, ATCC) which were differentiated into mature adipocytes (see Appendix: Supplementary material), then cultured with a fluorescent glucose analogue, 6-(N-(7-nitrobenz-2-oxa-1,3-diazol-4-yl)amino)-6-deoxyglucose (6-NBDG), according to a previously described protocol (Jung et al., 2011). Briefly, triplicate wells of 3T3-L1 cells cultured in 24-well plates were used for experiments on days 8-15 post-induction of

differentiation. Cells were cultured in serum-free, low glucose (1.5 g/L) Dulbecco's Modified Eagles Medium (Sigma-Aldrich) for 2 h at 37 °C, 5% CO_2. Following aspiration of culture medium, cells were then incubated for 1 h at 37 °C, 5% CO_2, in 250 µL PBS containing 100 µM 6-NBDG in the presence or absence of 5 nM porcine insulin (Sigma-Aldrich), which is identical to canine insulin, or the different recombinant SCI analogues, isolated from bacterial periplasmic fractions. Cells were washed three times with 500 µL PBS and lysed using 650 µL per well 90% dimethyl-sulfoxide. Two hundred microlitres was transferred in triplicate to black 96-well plates and fluorescence measured using a SpectraMax M2 microplate reader (λ_{ex} = 466 nm, λ_{em} = 540 nm, cut-off = 530 nm). Fluorescence was compared between stimulated and unstimulated cells and between the different SCI analogues using one-way ANOVA, followed by the Student's *t*-test with the Bonferroni post-hoc correction applied (PASW Statistics for Windows). Adjusted values were considered significant at $P < 0.05$.

Results

Characterisation of recombinant single-chain insulin analogues

All constructs (rcPROINS, rcINS[GGGPGKR], rcINS[cIGF2C] and rcINS[hIGF2C]) were confirmed by sequencing in both pTAC-MAT-Tag-2 and pFLAG-MAT-Tag-ATS expression vectors. All constructs were induced to express recombinant protein simultaneously for 4 h and ELISA of bacterial whole cell lysates demonstrated the presence of recombinant protein expressing both MAT and FLAG epitopes (Fig. 2). Since the SCI analogues were designed flanked by FLAG at the 5' end and MAT at the 3' end, this was evidence that recombinant protein was being expressed as anticipated, with expression from the pFLAG-MAT-Tag-ATS vector greater than from the pTAC-MAT-Tag-2 vector. Western blotting was performed on the periplasmic fractions of bacteria transformed with the pFLAG-MAT-Tag-ATS constructs, confirming that the recombinant proteins were of the anticipated sizes (Fig.

3).

Binding of recombinant SCI analogues to insulin and IGF-1 receptors

To assess differential binding of the SCI analogues to the INSR and IGF-1R, a direct ELISA was initially performed. This demonstrated that biotinylated insulin and IGF-1 preferentially bound their cognate receptors (Fig. 4A). Although rcPROINS showed a degree of binding to the INSR and IGF-1R, binding to the INSR was greater and more selective, compared to binding to IGF-1R for the three SCI analogues assessed (Fig. 4A). Comparing the relative binding for ligands to rhINSR and rhIGF-1R, revealed ratios of 1.6:1 for rcPROINS, 4.9:1 for rcINS[GGGPGKR], 3.1:1 for rcINS[cIGF-2C] and 4.9:1 for rcINS[hIGF-2C], compared to 5.5:1 for insulin and 0.17:1 for IGF-1.

Dose-response curves for binding of each recombinant protein to rhINSR demonstrated that saturation was reached at approximately 5 nM (Fig. 4B). The dose-response curve for rcPROINS was shifted to the right, whilst the curves for all SCI analogues were similar. A competitive-inhibition ELISA against biotinylated insulin was performed to obtain comparative IC_{50} values for the binding of each rcINS to the insulin receptor (Fig. 4C). It was not possible to obtain an IC_{50} value for rcPROINS, since sufficient inhibition of the signal could not be achieved with the maximum concentration of recombinant protein available. The relative IC_{50} values for rcINS[cIGF-2C] and for rcINS[hIGF-2C] were similar, at 593 pM and 613 pM respectively. The lowest IC_{50} was demonstrated by rcINS[GGGPGKR], at 187 pM, suggesting a higher affinity for the insulin receptor compared to the rcINS[IGF-2C] constructs.

Stimulation of glucose uptake by recombinant SCI analogues

Fluorescent glucose uptake was not significantly different comparing unstimulated

cells to cells incubated with rcPROINS (Fig. 5). In contrast, fluorescent glucose uptake by cells incubated with porcine insulin, rcINS[GGGPGKR], rcINS[cIGF-2C] and rcINS[hIGF-2C] was significantly greater than in unstimulated cells ($P < 0.05$). While cells cultured with each SCI analogue demonstrated significantly greater fluorescence than with rcPROINS ($P < 0.05$), there was no significant difference comparing the three different recombinant SCI analogues.

Discussion

The present study developed a number of plasmid DNA constructs that could be used for prokaryotic expression of recombinant SCI analogues, where the insulin C-peptide was replaced with either a synthetic linker, canine IGF-2 C-peptide or human IGF2-C peptide. These SCI analogues were shown to be capable of binding to the INSR and stimulating glucose uptake in vitro.

Recombinant proteins produced in this study were expressed as epitope-tagged fusion proteins. Prokaryotic vectors were selected that produced recombinant proteins with a C-terminal metal-affinity tag. Such epitope-tagged recombinant proteins can be immobilised using metals such as nickel, which is useful for both detection and purification. A FLAG epitope was inserted upstream of the B-chain coding sequence, which also possessed an enterokinase cleavage site immediately before the start of the B-chain, so that this epitope could potentially be removed, if the presence of the FLAG peptide inhibited receptor binding.

Expression of each construct was assessed by both ELISA and Western blotting, demonstrating that recombinant proteins of the appropriate sizes were produced from both pTAC-MAT-Tag-2 and pFLAG-MAT-Tag-ATS vectors in *E. coli*. Expression from pTAC-MAT-Tag-2 resulted in production of recombinant protein for each rcINS construct, although

subsequent work demonstrated that this was primarily in the insoluble fraction (data not shown). Expression of recombinant protein in *E. coli* commonly results in aggregation and formation of inclusion bodies (Thomas and Baneyx, 1996). The reducing environment of the bacterial cytosol does not favour folding of eukaryotic protein, especially those reliant on disulphide bond formation (Mergulhao et al., 2004), such as insulin (Williams et al., 1982).

Unlike the bacterial cytosol, the periplasm (the space between the inner cytoplasmic membrane and external outer membrane of Gram-negative bacteria) provides an oxidising environment which is more favourable for protein folding and disulphide bond formation (Baneyx and Mujacic, 2004). Therefore, the pFLAG-MAT-Tag-ATS vector was employed in an attempt to increase the yield of soluble protein. The pFLAG-MAT-Tag-ATS vector encodes the outer membrane protein A signal peptide (OmpA) and incorporation of this sequence at the N-terminus targets recombinant protein to the periplasm, where the OmpA is cleaved by signal peptidase as the recombinant protein crosses the bacterial inner cytoplasmic membrane (Freudl et al., 1987). Western blot analysis of periplasmic preparations, isolated for use in downstream assays demonstrated the molecular weight differences between the different rcINS proteins (Fig. 3).

Receptor-binding assays were developed to assess the different SCI analogues against rhINSR and rhIGF-1R, with biotinylated insulin and IGF-1 used as control ligands. Although human recombinant receptors were used, this was considered appropriate since canine IGF-1[2] and human IGF-1[3] share an identical sequence and canine insulin[4] and human insulin[5] differ by only one amino acid in the B chain (B30A/T). However, it should be noted that these studies

[2] See: http://www.uniprot.org/uniprot/P33712
[3] See: http://www.uniprot.org/uniprot/Q9NP10
[4] See: http://www.uniprot.org/uniprot/P01321
[5] See: http://www.uniprot.org/uniprot/P01308

were undertaken with heterologous receptors, which might not represent the situation with autologous canine receptors. Initial studies established the working range of the assays with a receptor concentration of 2–4 μg/mL found to be optimal, resulting in sensitivity for ligand binding down to approximately 0.1 nM. It was important to assess binding to rhIGF-1R as well as to rhINSR, since an insulin analogue might have the potential for increased affinity, resulting from changes to the peptide sequence, with subsequent mitogenic activity and increased oncogenic potential (Vajo et al., 2001).

Detection using anti-FLAG antibody confirmed that all SCI analogues were able to bind to both rhINSR and rhIGF-1R. Binding of rcPROINS to rhINSR resulted in a significantly weaker signal compared to each of the SCI analogues, suggesting lower affinity for the receptor. This is consistent with other studies, which demonstrate that proinsulin has relative affinity of 1–2% for INSR compared to insulin (Lee et al., 2000). There was no significant difference in signal for rhINSR binding comparing the different SCI analogues. Incubation with rhIGF-1R gave significantly reduced signals for rcPROINS and for each SCI analogue, compared to binding to rhINSR, and there was no significant difference in rhIGF-1R signal within the rcPROINS/rcINS group.

The results of the receptor-binding assays suggest that all SCI analogues demonstrate greater affinity for the rhINSR than for the rhIGF-1R, with rcINS[GGGPGKR] and rcINS[hIGF-2C] showing relative binding similar to that demonstrated by insulin. Using a competitive-inhibition ELISA against INSR, the rcINS[GGGPGKR] analogue demonstrated the highest relative affinity (IC_{50} = 187 pM), followed by rcINS[cIGF-2C] (IC_{50} = 593 pM) and rcINS[cIGF-2C] (IC_{50} = 613 pM). It was not possible to calculate IC_{50} for rcPROINS since sufficient inhibition could not be achieved, even using a concentration of 20 nM. This indicates

that each of the SCI analogues showed much greater affinity than rcPROINS. The two insulin/IGF-2 C-peptide chimaeric proteins demonstrated similar relative affinity for rhINSR, which is unsurprising since they differ by only two residues (Fig. 1B).

There are several other studies describing binding characteristics of SCI analogues. Lee et al. (2000), who developed a human SCI analogue containing the GGGPGKR linker, compared its receptor binding with both insulin and proinsulin, reporting an affinity for the INSR of 28% compared to native insulin, and 1350% that of proinsulin. In a more recent study investigating over 30 different SCI analogues, it was concluded that intermediate linking peptides of 7-10 residues, composed primarily of glycine residues (to promote molecular flexibility) along with a C-terminal arginine, demonstrate the greatest INSR affinities and bioactivity (Rajpal et al., 2009). Indeed, a SCI analogue with a hexapeptide linking sequence (GGGPRR) has demonstrated enhanced INSR affinity of 130% compared to native insulin, although in that particular molecule the A8:threonine residue was also replaced with histidine (Hua et al., 2008).

We are not aware of any studies that have investigated SCI analogues based on the concept of an insulin/IGF-2 C-peptide chimaera, although there has been a report of an insulin/IGF-1 C-peptide chimaera (Kristensen et al, 1995). The binding affinity for that molecule compared favourably with insulin, and was reported to be between 55-94%. This was surprising since the presence of the linking peptide was predicted to limit the flexibility of the insulin domains necessary for receptor binding, and it was also expected to impair the important A1:glycine residue essential for receptor binding (Pullen et al., 1976). It was proposed that the C-peptide of IGF-1 interacted directly with a conserved domain in the INSR since this receptor and the IGF-1R are similar. This is unlikely to be the case with an

insulin/IGF-2 C-peptide chimaera since the IGF-2R belongs to a functionally different receptor class.

In glucose uptake assays, adipocytes derived from 3T3-L1 cells incubated with porcine insulin, rcINS[GGGPGKR], rcINS[cIGF-2C] or rcINS[hIGF-2C] all resulted in significantly higher fluorescence (suggesting GLUT4 mediated 6-NBDG uptake) compared to unstimulated cells. All SCI analogues resulted in comparable 6-NBDG uptake, which was significantly greater than that seen with rcPROINS. This indicates that substitution of the proinsulin C-peptide for the various linker peptides resulted in biologically-active molecules.

Conclusions

The present study has demonstrated that it is possible to produce recombinant canine SCI analogues that are capable of INSR binding and stimulating glucose uptake in cells, without the need for post-translational processing. This work paves the way for production of recombinant canine insulin analogues that could be scaled up, with a view to developing novel therapeutics for canine diabetes.

Conflict of interest statement

None of the authors of this paper has any financial or personal relationship with other people or organizations that could inappropriately influence or bias the content of the paper. This work was undertaken as part of a BBSRC CASE studentship with MSD Animal Health as the industrial sponsor. MSD Animal Health had no involvement in the study design, collection, analysis and interpretation of data, writing of this manuscript or the decision to submit the article for publication.

Acknowledgements

We are grateful to BBSRC for funding this industrial CASE studentship (BB/E527798/1) and to MSD Animal Health for their participation as the industrial partner.

Appendix: Supplementary material

Supplementary data to this article can be found online at doi:xxx

References

Baneyx, F., Mujacic, M., 2004. Recombinant protein folding and misfolding in *Escherichia coli*. Nature Biotechnology 22, 1399-1408.

Boari, A., Barreca, A., Bestetti, G.E., Minuto, F., Venturoli, M., 1995. Hypoglycemia in a dog with a leiomyoma of the gastric wall producing an insulin-like growth factor II-like peptide. European Journal of Endocrinology 132, 744-750.

Borgono, C.A., Zinman, B., 2012. Insulins: Past, present, and future. Endocrinology and Metabolism Clinics of North America 41, 1-24.

Catchpole, B., Kennedy, L.J., Davison, L.J., Ollier, W.E., 2008. Canine diabetes mellitus: from phenotype to genotype. Journal of Small Animal Practice 49, 4-10.

Chan, S.J., Steiner, D.F., 2000. Insulin through the ages: Phylogeny of a growth promoting and metabolic regulatory hormone. American Zoologist 40, 213-222.

Christensen, T., Dalboge, H., Snel, L., 1991. Postbiosynthesis modification: Human growth hormone and insulin precursors. Bioprocess Technology 13, 206-221.

DeChiara, T.M., Efstratiadis, A., Robertson, E.J., 1990. A growth-deficiency phenotype in heterozygous mice carrying an insulin-like growth factor II gene disrupted by targeting. Nature 345, 78-80.

Freudl, R., Schwarz, H., Degen, M., Henning, U., 1987. The signal sequence suffices to direct export of outer membrane protein OmpA of *Escherichia coli* K-12. Journal of Bacteriology 169, 66-71.

Hua, Q.X., Nakagawa, S.H., Jia, W., Huang, K., Phillips, N.B., Hu, S.Q., Weiss, M.A., 2008. Design of an active ultrastable single-chain insulin analog: Synthesis, structure, and therapeutic implications. Journal of Biological Chemistry 283, 14703-14716.

Jung, D.W., Ha, H.H., Zheng, X., Chang, Y.T., Williams, D.R., 2011. Novel use of fluorescent glucose analogues to identify a new class of triazine-based insulin mimetics possessing useful secondary effects. Molecular Biosystems 7, 346-358

Kristensen, C., Andersen, A.S., Hach, M., Wiberg, F.C., Schaffer, L., Kjeldsen, T., 1995. A single-chain insulin-like growth factor I/insulin hybrid binds with high affinity to the insulin receptor. Biochemical Journal 305, 981-986.

Lee, H.C., Kim, S.J., Kim, K.S., Shin, H.C., Yoon, J.W., 2000. Remission in models of type 1 diabetes by gene therapy using a single-chain insulin analogue. Nature 408, 483-488.

LeRoith, D., 2004. Non-islet cell hypoglycemia. Annals of Endocrinology 65, 99-103.

Liu, J.P., Baker, J., Perkins, A.S., Robertson, E.J., Efstratiadis, A., 1993. Mice carrying null mutations of the genes encoding insulin-like growth factor I (Igf-1) and type 1 IGF receptor (Igf1r). Cell 75, 59-72.

Mergulhao, F.J., Taipa, M.A., Cabral, J.M., Monteiro, G.A., 2004. Evaluation of bottlenecks in proinsulin secretion by *Escherichia coli*. Journal of Biotechnology 109, 31-43.

Peavy, D.E., Brunner, M.R., Duckworth, W.C., Hooker, C.S., Frank, B.H., 1985. Receptor binding and biological potency of several split forms (conversion intermediates) of human proinsulin. Studies in cultured IM-9 lymphocytes and in vivo and in vitro in rats. Journal of Biological Chemistry 260, 13989-13994.

Pullen, R.A., Lindsay, D.G., Wood, S.P., Tickle, I.J., Blundell, T.L., Wollmer, A., Krail, G., Brandenburg, D., Zahn, H., Gliemann, J., Gammeltoft, S., 1976. Receptor-binding region of insulin. Nature 259, 369-373.

Rajpal, G., Liu, M., Zhang, Y., Arvan, P., 2009. Single-chain insulins as receptor agonists. Molecular Endocrinology 23, 679-688.

Riggs, A.D., Itakura, K., 1979. Synthetic DNA and medicine. American Journal of Human Genetics 31, 531-538.

Rucinsky, R., Cook, A., Haley, S., Nelson, R., Zoran, D.L., Poundstone, M., 2010. AAHA diabetes management guidelines for dogs and cats. Journal of the American Animal Hospital Association 46, 215-224.

Thomas, J.G., Baneyx, F., 1996. Protein misfolding and inclusion body formation in recombinant *Escherichia coli* cells overexpressing heat-shock proteins. Journal of Biological Chemistry 271, 11141-11147.

Vajo, Z., Fawcett, J., Duckworth, W.C., 2001. Recombinant DNA technology in the treatment of diabetes: Insulin analogs. Endocrinology Reviews 22, 706-717.

Williams, D.C., Van Frank, R.M., Muth, W.L., Burnett, J.P., 1982. Cytoplasmic inclusion bodies in *Escherichia coli* producing biosynthetic human insulin proteins. Science 215, 687-689.

Zini, E., Glaus, T.M., Minuto, F., Arvigo, M., Hauser, B., Reusch, C.E., 2007. Paraneoplastic hypoglycemia due to an insulin-like growth factor type-II secreting hepatocellular carcinoma in a dog. Journal of Veterinary Internal Medicine 21, 193-195.

Figure legends

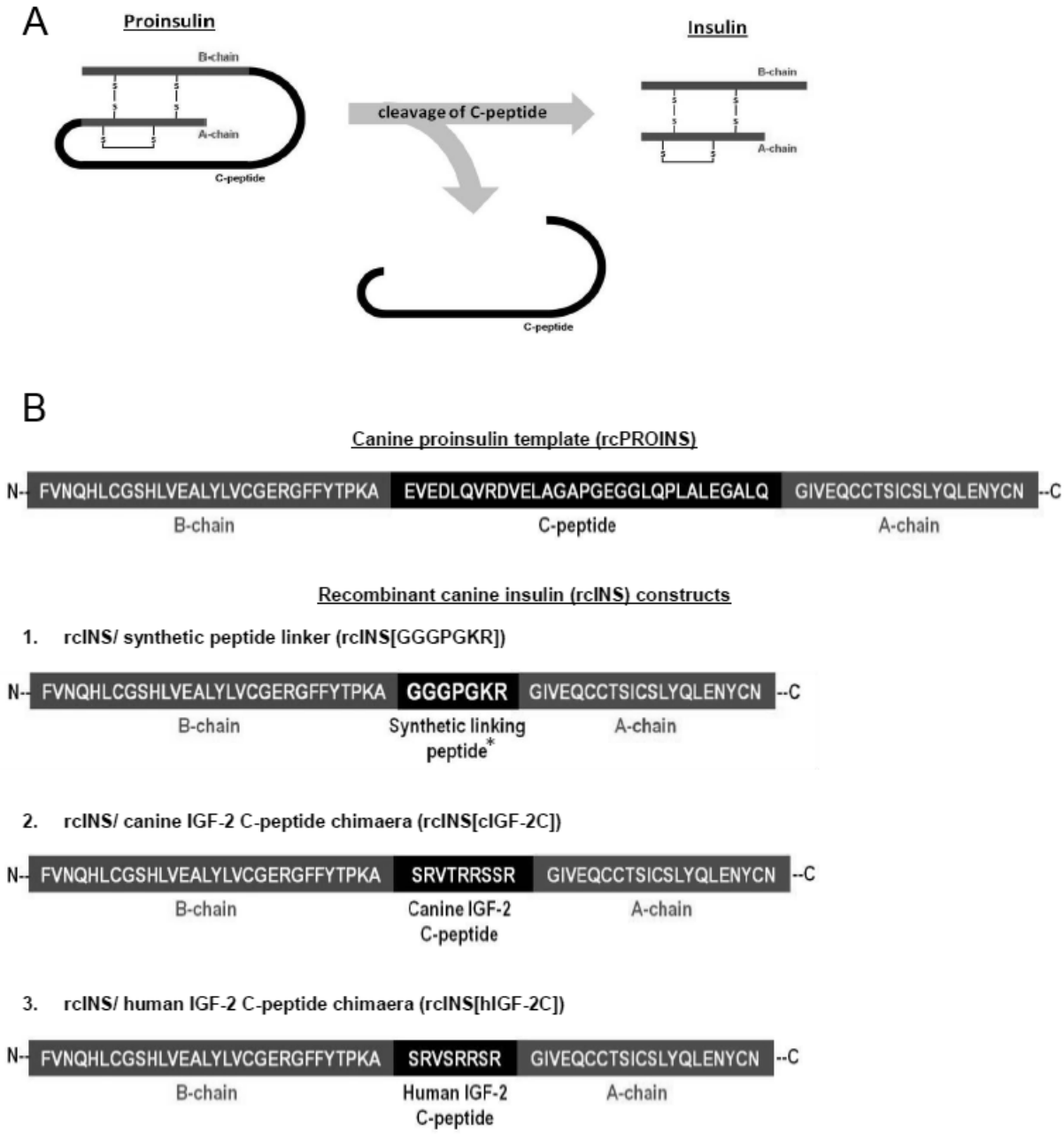

Fig. 1. (A) Post-translational modification of proinsulin to yield the biologically-active insulin and C-peptide. (B) Details of single chain insulin analogues adapted from recombinant canine proinsulin (rcPROINS) for the present study. Three different recombinant canine insulin analogues (rcINS) were generated, where the insulin C-peptide was substituted with different linking peptide sequences.

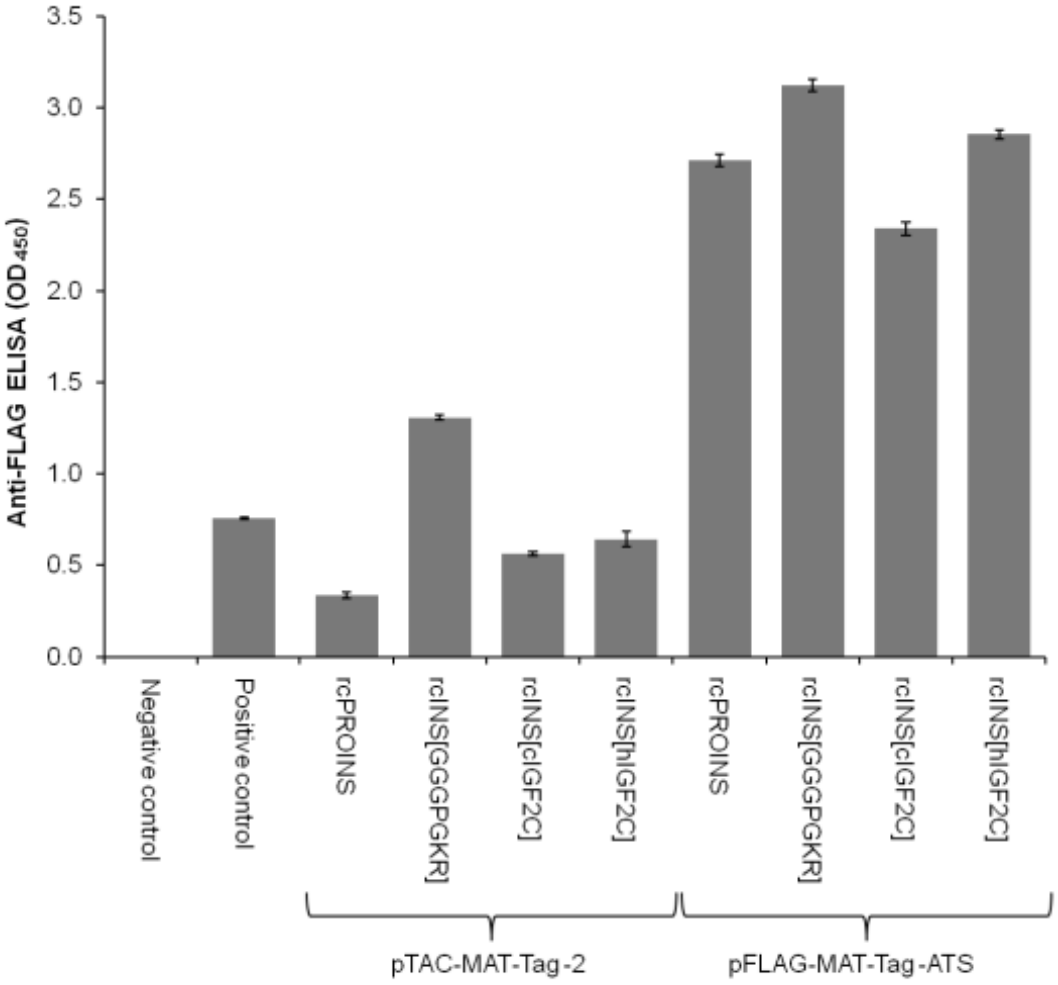

493

494 Fig. 2. Detection of FLAG-tagged recombinant protein. BL-21(T1) *Escherichia coli* were
495 transformed with each rcINS construct in one of two expression vectors. After induction of
496 expression, bacterial lysates were prepared and analysed by ELISA, using nickel-coated plates
497 to capture proteins expressing a metal-affinity tag and detected using an anti-FLAG antibody.
498 Absorbance is shown as the mean ± standard error of the mean (SEM) of triplicate wells
499 following subtraction of background (lysis buffer only). Negative control is lysate from
500 bacteria transformed with wild-type pTAC-MAT-Tag-2 plasmid DNA. Positive control is lysate
501 from bacteria transformed with pFLAG-MAT-Tag-ATS+BAP. The experiment was repeated
502 with similar results.

503

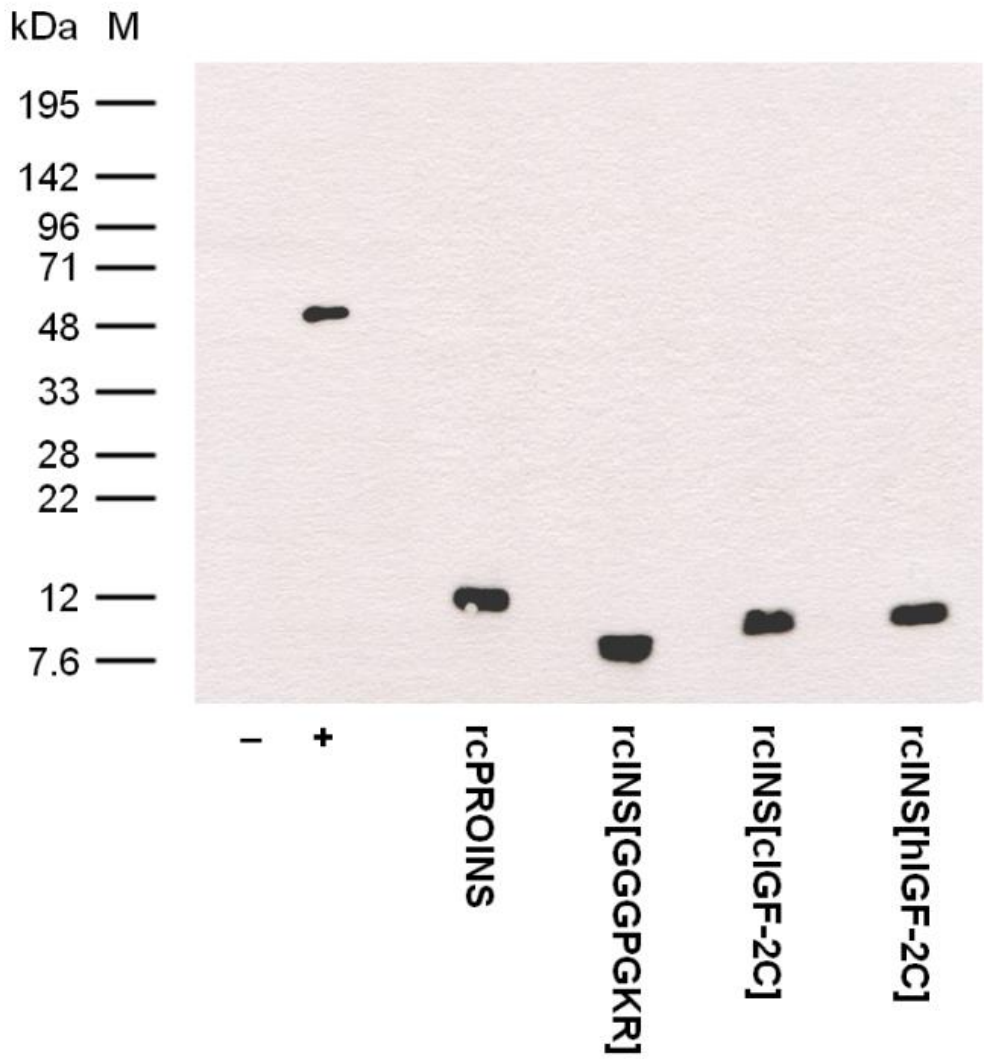

504

505 Fig. 3. Western blotting of FLAG-tagged rcINS isolated from bacterial periplasmic fractions.
506 BL-21 (T1) *Escherichia coli* were transformed with pFLAG-MAT-Tag-ATS plasmid DNA
507 containing the indicated constructs. After induction of expression, bacteria were subjected to
508 osmotic lysis and periplasmic samples analysed by Western blotting, using an anti-FLAG
509 antibody, detected by enhanced chemiluminescence. The negative control (-) is from bacteria
510 transformed with wild-type pTAC-MAT-Tag-2 vector and the positive control (+) is from
511 bacteria transformed with pFLAG-MAT-Tag-ATS+BAP (anticipated size of bacterial alkaline
512 phosphatase ~50kDa). M, molecular weight marker.

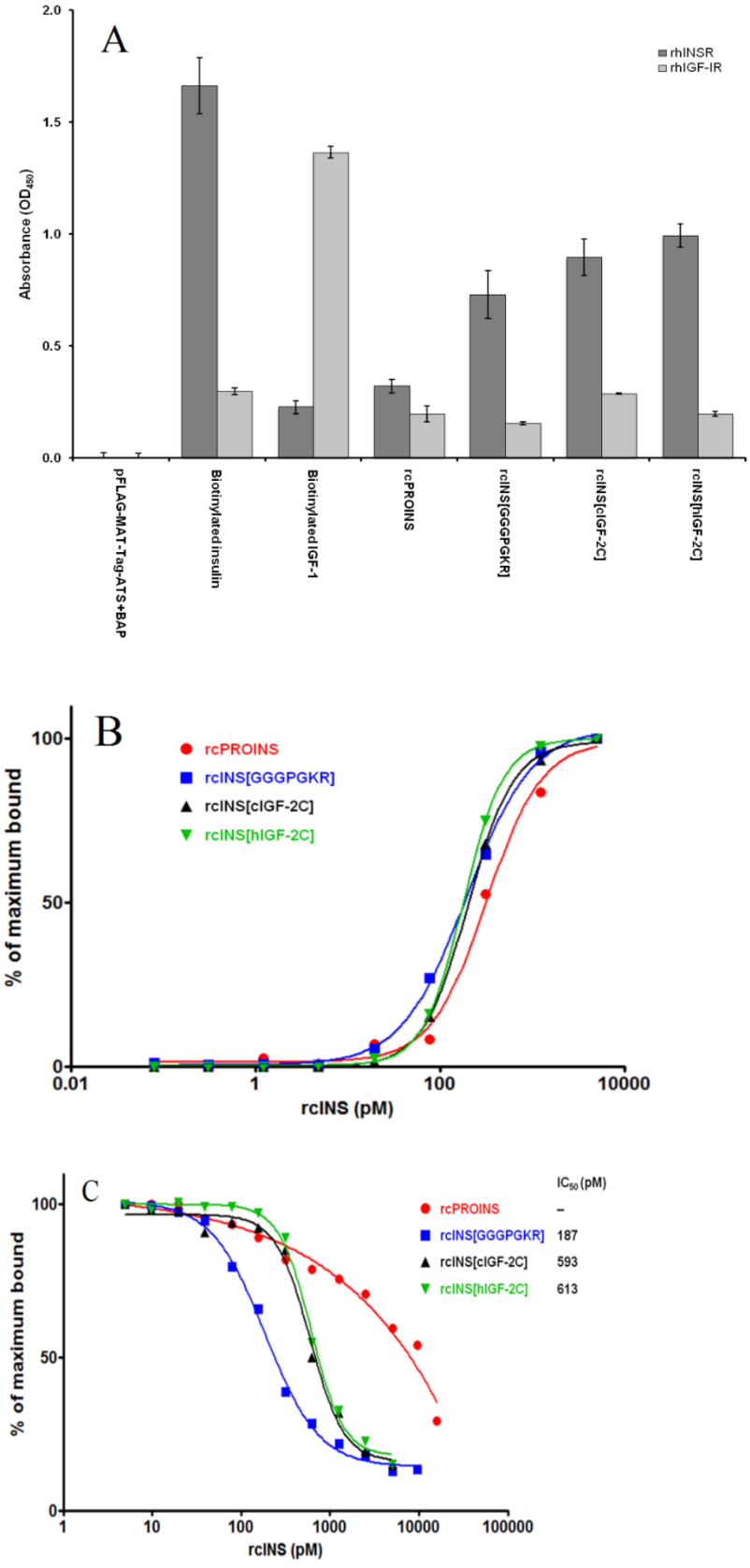

513

514 Fig. 4. (A) Binding of rcINS constructs to INSR and IGF-1R. ELISA wells were coated with 4

515 µg/mL rhINSR or rhIGF-1R. Biotinylated bovine insulin, biotinylated human IGF-1 or

516 periplasmic fractions of the indicated constructs (all 5 nM) were added and binding detected
517 using either streptavidin-HRP or anti-FLAG HRP antibody. Absorbance is shown as the mean
518 ± standard error of the mean (SEM) of triplicate wells. (B) Dose-response curve for binding of
519 rcINS constructs to INSR. (C) Competition-ELISA for binding of rcINS constructs to INSR.
520 Increasing concentrations of rcINS protein were co-cultured in rhINSR coated plates in the
521 presence of 3 nM biotinylated bovine insulin, with binding detected using streptavidin-HRP.
522

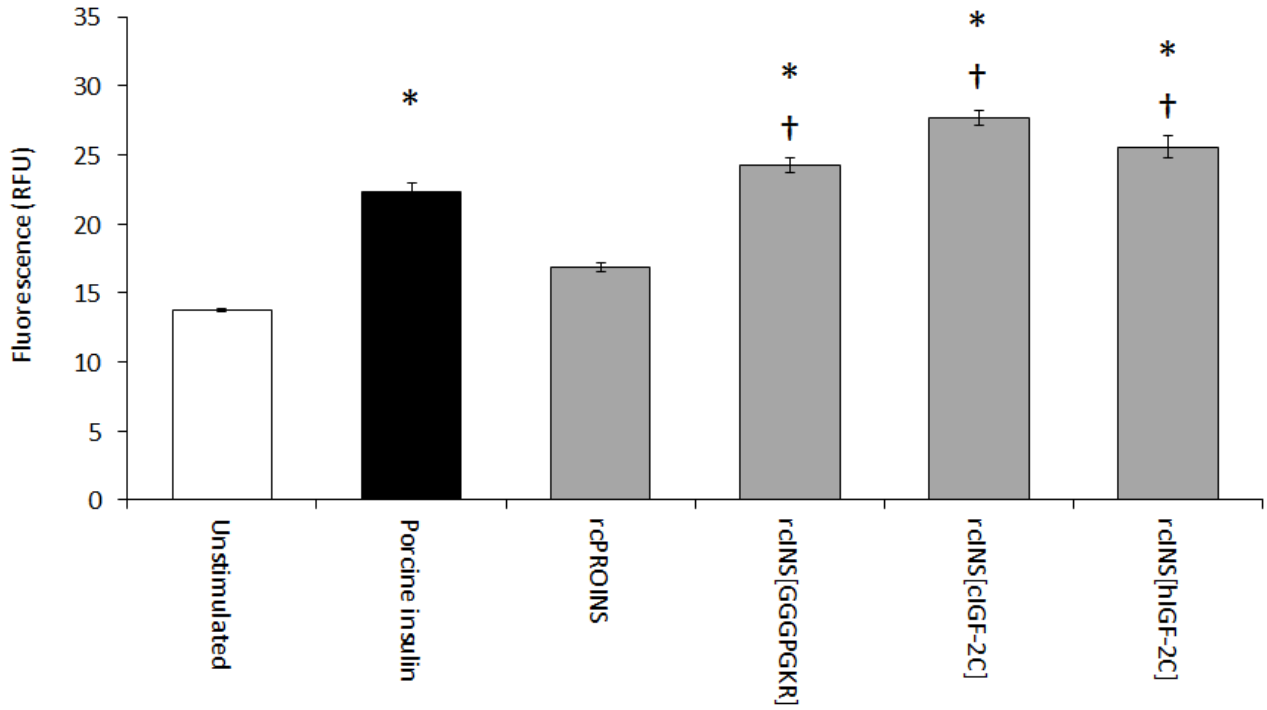

523

524 Fig. 5. Assessment of insulin-stimulated glucose uptake in 3T3-L1 adipocytes. 3T3-L1
525 adipocytes were serum-starved in low-glucose DMEM for 2 h prior to incubation with
526 fluorescent glucose analogue 6-NBDG for 1 h in the presence of 5 nM porcine insulin,
527 recombinant canine proinsulin (rcPROINS) or the indicated recombinant canine insulin
528 analogues. Cells were lysed and fluorescence measured (λ_{ex} = 466 nm, λ_{em} = 540 nm, cut-off
529 = 530 nm). Results represent the mean of triplicate samples ± SEM. The Student's *t* test was
530 used to compare fluorescence of stimulated cells to unstimulated cells (* P <0.05) and to
531 compare recombinant insulin analogues to rcPROINS († P <0.05).

532

Appendix: Supplementary Table 1

Restriction endonuclease sites shown underlined; coding sequences in bold refer to explanation in target column.

Primer name	Target	Primer sequence		Amplicon length (bp)
PROINS pTACMAT *Eco*RI/*Sph*I	Canine proinsulin coding sequence with additional restriction site *Eco*RI for cloning	For:	GAATTCGTTAACCAGCACCTG	268
	Canine proinsulin coding sequence with additional restriction site *Sph*I for cloning	Rev:	GCATGCCGTTGCAGTAATTCTCCAG	
INS A CORE	Amplification of canine insulin A chain. Used with PROINS pTACMAT *Sph*I REV.	For:	GGCATCGTGGAGCAGTGC	70
INS B CORE	Amplification of canine insulin B chain. Used with PROINS pTACMAT *Eco*RI FOR	Rev:	GGCCTTAGGCGTGTAGAAG	93
INS A LINK	Modified INS A CORE primer to generate synthetic linker sequence (in bold). Contains *Xma*I restriction site. Used with PROINS pTACMAT *Sph*I REV	For:	CCCGGGTAAGAGAGGCATCGTGGAGCAGTGC	83
INS B LINK	Modified INS B CORE primer to generate synthetic linker sequence (in bold). Contains *Xma*I restriction site. Used with PROINS pTACMAT *Eco*RI FOR	Rev:	ATACCCGGGCCACCACCTGCCTTAGGCGTGTAG	110
INSA cIGF2C	Amplification of canine insulin A chain and part of canine IGF-2 C peptide (in bold). Contains *Bgl*II site. Used with PROINS pTACMAT *Sph*I REV	For:	AGATCTAGCCGTGGCATCGTGGAGCAGTGC	82
INSB cIGF2C	Amplification of canine insulin B chain and part of canine IGF-2 C peptide (in bold). Contains *Bgl*II site. Used with PROINS pTACMAT *Eco*RI FOR	Rev:	GATCTGCGAGTTACGCGAGAGGCCTTAGGCGTGTAGAAG	113
INSA hIGF2C	Amplification of canine insulin A chain and part of human IGF-2 C peptide (in bold). Contains *Xba*I site.Used with PROINS pTACMAT *Sph*I REV	For:	TCTAGACGCAGCCGTGGCATCGTGGAGCAGTGC	85
INSB hIGF2C	Amplification of canine insulin B chain and part of human IGF-2 C peptide (in bold). Contains *Xba*I site. Used with PROINS pTACMAT *Eco*RI FOR	Rev:	GATCTAGACACGCGGCTGGCCTTAGGCGTGTAGAAG	110

For, forward; Rev, reverse; bp, base pairs.

Separate coding sequences for canine insulin A-chain and B-chain were generated by PCR, using pSC-A/rcPROINS pDNA as template. The reverse primer for the insulin B chain, and the forward primer for the insulin A-chain incorporated the additional coding sequence for the synthetic peptide linker (GGGPGKR) as well as for *XmaI*, to facilitate ligation.

PCR product for **insulin B-chain** + **synthetic peptide linker** (INSB/GGG) coding sequence (110 bp). Primer pair: PROINS pTACMAT *EcoRI* For/ INS B LINK Rev
Incorporated 5' *EcoRI* site and 3' *XmaI* site:

EcoRI *XmaI*

```
GAATTCGTTAACCAGCACCTGTGTGGCTCCCACCTGGTAGAGGCTCTGTACCTGGTGTGCGGGGAGCGCGGCTTCTTCTACACGCCTAAGGCAGGTGGTGGCCCGGGTAT
CTTAAGCAATTGGTCGTGGACACACCGAGGGTGGACCATCTCCGAGACATGGACCACACGCCCCTCGCGCCGAAGAAGATGTGCGGATTCCGTCCACCACCGGGCCCATA
```

PCR product for **synthetic peptide linker** + **insulin A-chain** (PKGR/INSA) coding sequence (83 bp). Primer pair: INS A LINK For/ PROINS pTACMAT *SphI* Rev
Incorporated 5' *XmaI* site and 3' *SphI* site:

XmaI *SphI*

```
CCCGGGTAAGAGAGGCATCGTGGAGCAGTGCTGCACCAGCATCTGCTCCCTCTACCAGCTGGAGAATTACTGCAACGGCATGC
GGGCCCATTCTCTCCGTAGCACCTCGTCACGACGTGGTCGTAGACGAGGGAGATGGTCGACCTCTTAATGACGTTGCCGTACG
```

1. The complete coding sequence for rcINS[GGGPGKR] was constructed via ligation of sticky ends generated following digestion of coding sequences with *XmaI*.

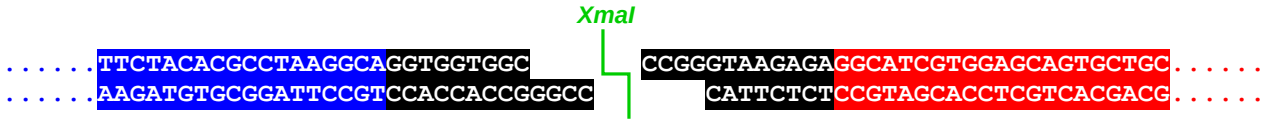

2. rcINS[GGGPGKR] following ligation:

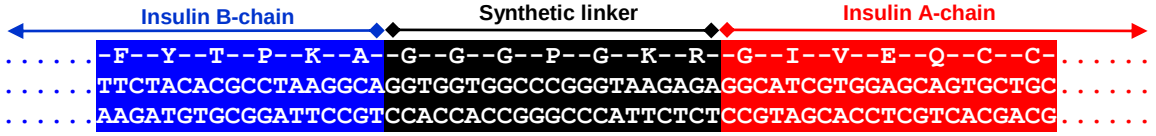

Suppl Fig. 1. Generation of rcINS/ synthetic peptide linker (rcINS[GGGPGKR])
Coding sequences for insulin B-chain highlighted in blue, for linking peptide sequence in black, and for insulin A-chain highlighted in red. Non-coding sequences are not highlighted. Primer binding sites are shown underlined. Restriction sites shown in ***green***. Primer sequences are given in Supplementary Table 1.

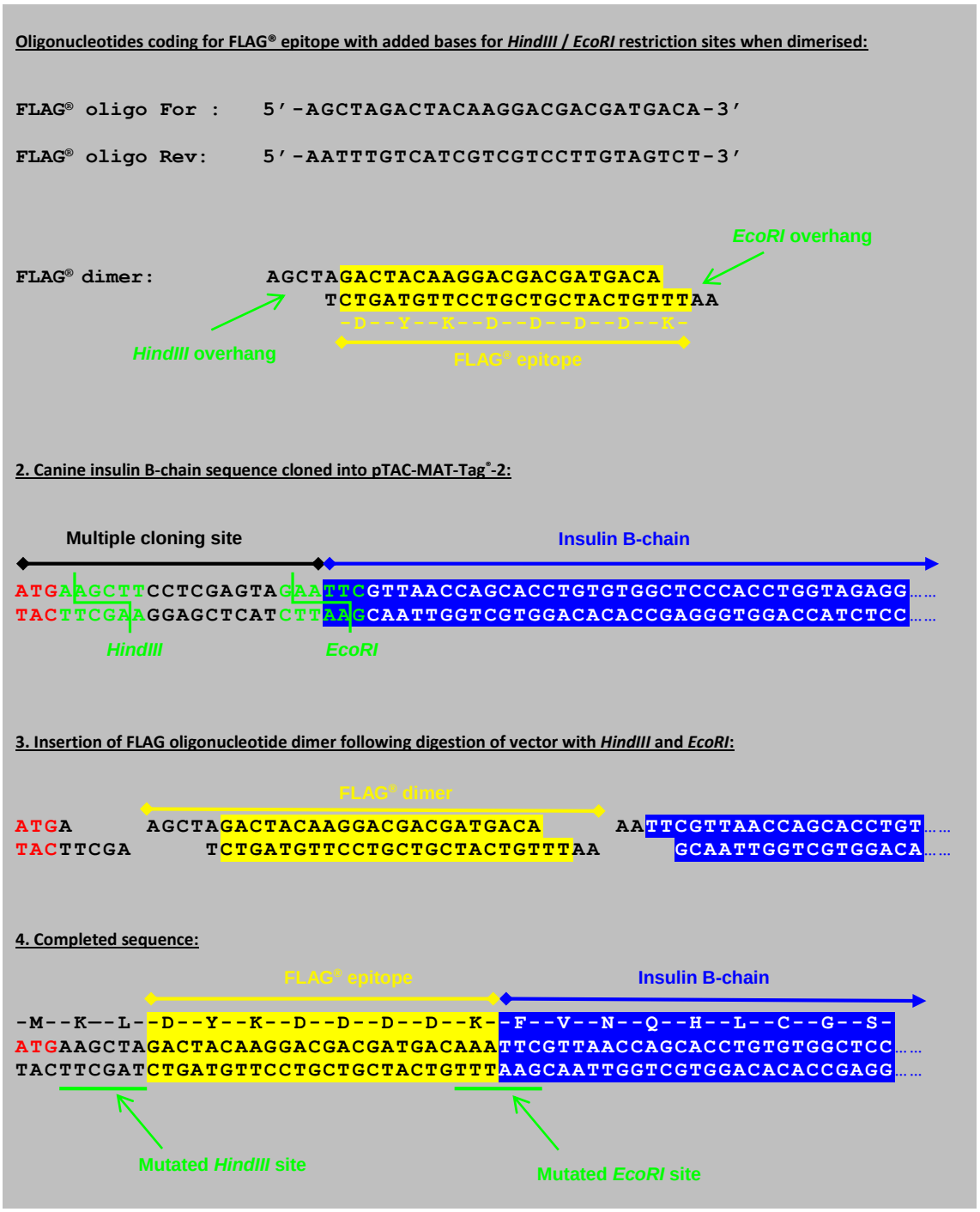

Suppl. Fig. 2. Schematic illustrating insertion of FLAG® coding sequence into pTAC-MAT-Tag®-2/rcPROINS and pTAC-MAT-Tag®-2/rcINS[GGGPGKR]
FLAG oligonucleotides were annealed to form a dimer and then ligated into the pTAC-MAT-Tag®-2 vector containing rcPROINS or rcINS[GGGPGKR] which had been digested with *HindIII* and *EcoRI*. Recognition sites shown in green, start codon in red.

Separate coding sequences for canine insulin A-chain and B-chain were generated by PCR, using pSC-A/rcPROINS or pTAC-MAT-Tag®-2/FLAG®-rcPROINS pDNA respectively as template. The reverse primer for the insulin B chain, and the forward primer for the insulin A-chain incorporated the additional coding sequence for the canine IGF-2 C-peptide (cIGF-2C) as well as for *BglII*, to facilitate ligation.

PCR product for **insulin B-chain** + **canine IGF-2 C-peptide** coding sequence incorporating the FLAG® epitope (141 bp). Primer pair: FLAG® For/ INS B cIGF2C Rev
Incorporated 5' *HindIII* site and 3' *BglII* site (3' terminal T/A added by *Taq* DNA polymerase)

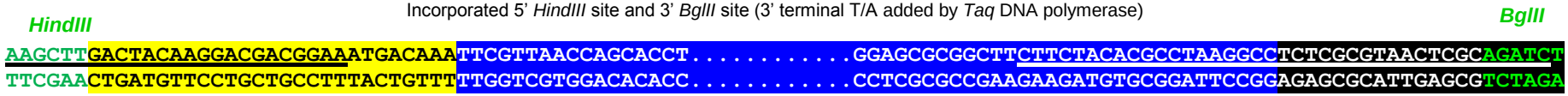

PCR product for **canine IGF-2 C-peptide** + **insulin A-chain** coding sequence (82 bp). Primer pair: INS A cIGF2C For/ PROINS pTACMAT *SphI* Rev
Incorporated 5' *BglII* site and 3' *SphI* site:

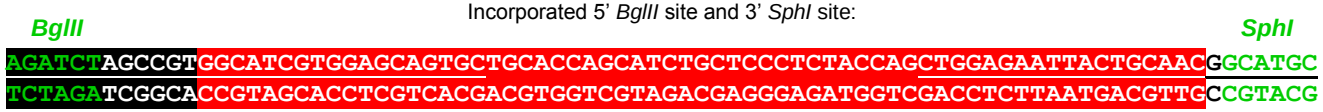

1. The complete coding sequence for rcINS[cIGF-2C] was constructed via ligation of sticky ends generated following digestion of both coding sequences with *BglII*.

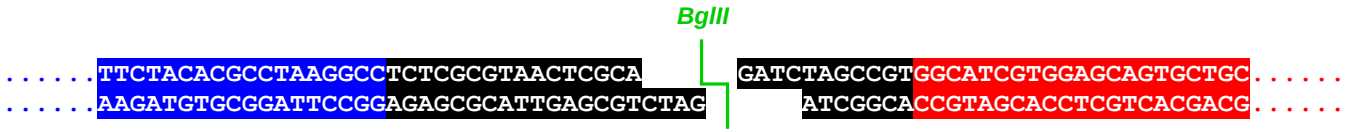

2. rcINS[cIGF-2C] following ligation:

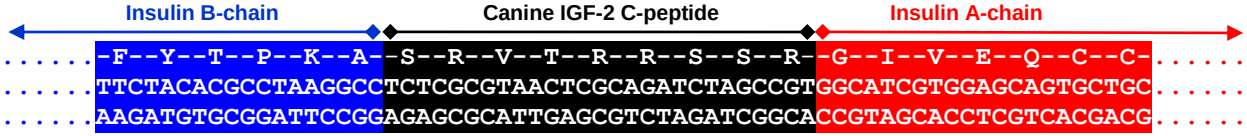

Suppl. Fig. 3. Generation of rcINS/ canine IGF-2 C-peptide chimaera (rcINS[cIGF2-C])
Coding sequences for insulin B-chain highlighted in blue, for linking peptide sequence in black, and for insulin A-chain highlighted in red. FLAG® epitope coding sequence highlighted in yellow. Non-coding sequences are not highlighted. Primer binding sites are shown underlined. Restriction sites shown in ***green***. Primer sequences are given in Supplementary Table 1.

Separate coding sequences for canine insulin A-chain and B-chain were generated by PCR, using pSC-A/rcPROINS or pTAC-MAT-Tag®-2/FLAG®-rcPROINS pDNA respectively as template. The reverse primer for the insulin B chain, and the forward primer for the insulin A-chain incorporated the additional coding sequence for the human IGF-2 C-peptide (hIGF-2C) as well as for *XbaI*, to facilitate ligation.

PCR product for **insulin B-chain** + **human IGF-2 C-peptide** coding sequence incorporating the FLAG® epitope (135 bp). Primer pair: FLAG® For/ INS B hIGF2C Rev
Incorporated 5' *EcoRI* site and 3' *XbaI* site (3' terminal T/A added by *Taq* DNA polymerase)

HindIII *XbaI*

```
AAGCTTGACTACAAGGACGACGGAAATGACAAATTCGTTAACCAGCACCT.............GGAGCGCGGCTTCTTCTACACGCCTAAGGCCAGCCGCGTGTCTAGA
TTCGAACTGATGTTCCTGCTGCCTTTACTGTTTTTGGTCGTGGACACACC.............CCTCGCGCCGAAGAAGATGTGCGGATTCCGGTCGGCGCACAGATCT
```

PCR product for **human IGF-2 C-peptide** + **insulin A-chain** coding sequence (85 bp). Primer pair: INS A hIGF2C/ PROINS pTACMAT *SphI* Rev
Incorporated 5' *XbaI* site and 3' *SphI* site:

XbaI *SphI*

```
TCTAGACGCAGCCGTGGCATCGTGGAGCAGTGCTGCACCAGCATCTGCTCCCTCTACCAGCTGGAGAATTACTGCAACGGCATGC
AGATCTGCGTCGGCACCGTAGCACCTCGTCACGACGTGGTCGTAGACGAGGGAGATGGTCGACCTCTTAATGACGTTGCCGTACG
```

1. The complete coding sequence for rcINS[hIGF-2C] was constructed via ligation of sticky ends generated by digestion of both coding sequences with *XbaI*.

XbaI

```
......TTCTACACGCCTAAGGCCAGCCGCGTGT    CTAGACGCAGCCGTGGCATCGTGGAGCAGTGCTGC......
......AAGATGTGCGGATTCCGGTCGGCGCACAGATC    TGCGTCGGCACCGTAGCACCTCGTCACGACG......
```

2. rcINS/hIGF-2C following ligation:

Insulin B-chain — Human IGF-2 C-peptide — Insulin A-chain

```
......-F--Y--T--P--K--A--S--R--V--S--R--R--S--R--G--I--V--E--Q--C--C-......
......TTCTACACGCCTAAGGCCAGCCGCGTGTCTAGACGCAGCCGTGGCATCGTGGAGCAGTGCTGC......
......AAGATGTGCGGATTCCGGTCGGCGCACAGATCTGCGTCGGCACCGTAGCACCTCGTCACGACG......
```

Suppl. Fig. 4. Generation of rcINS/ human IGF-2 C-peptide chimaera (rcINS[hIGF2-C])
Coding sequences for insulin B-chain highlighted in blue, for linking peptide sequence in black, and for insulin A-chain highlighted in red. FLAG® epitope coding sequence highlighted in yellow. Non-coding sequences are not highlighted. Primer binding sites are shown underlined. Restriction sites shown in ***green***. Primer sequences are given in Supplementary Table 1.

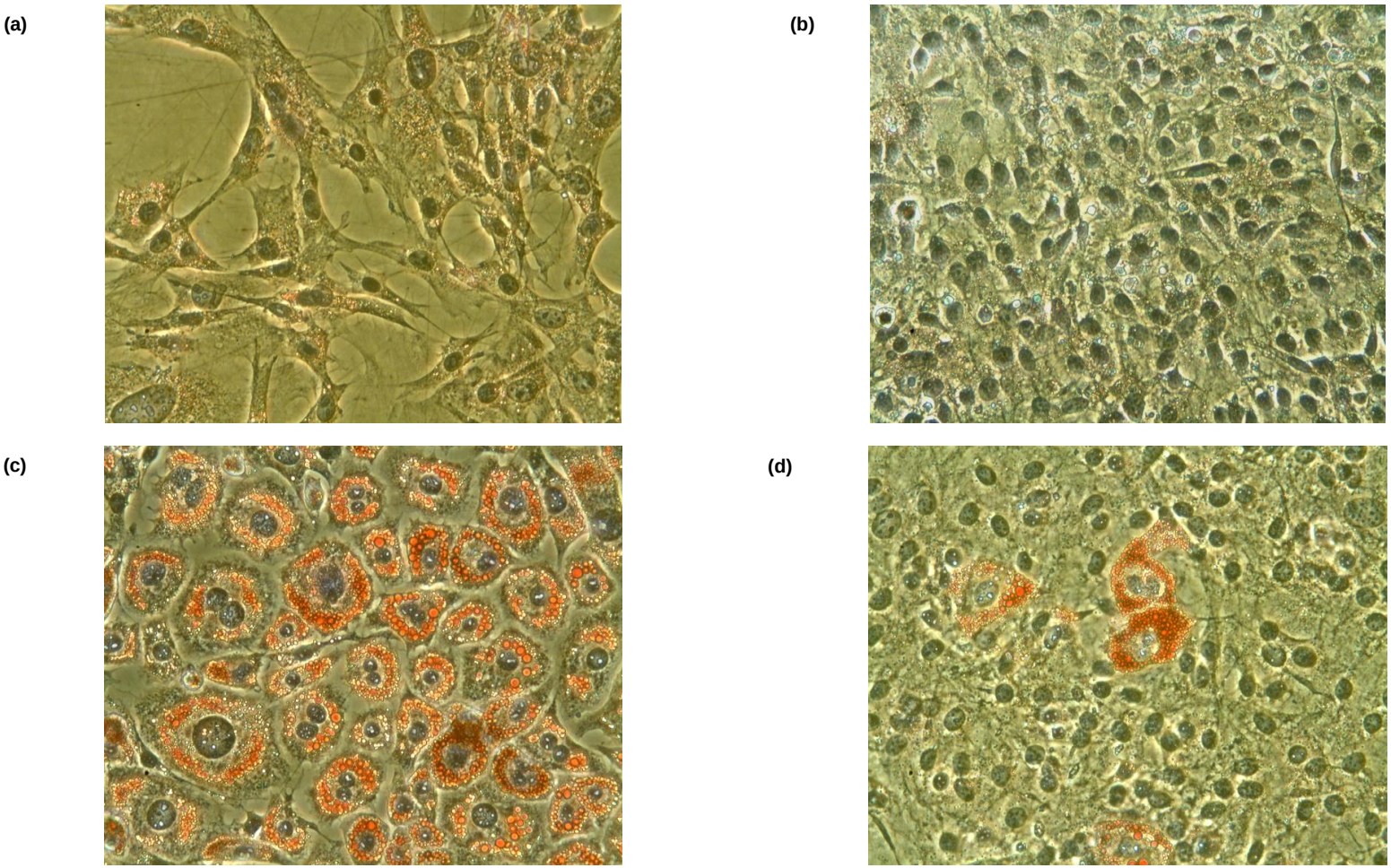

Suppl Fig. 5 Murine fibroblasts were differentiated into adipocytes

Murine fibroblasts (3T3-L1) were seeded at a density of 1 x 10^5 cells per well in 24-well tissue culture plates. After growing to confluency in DMEM/ 10% bovine calf serum, cells were cultured for another 48 h before induction of adipogenesis was induced with insulin, IBMX and dexamethasone in DMEM/ 10% FBS (day 0). Adipocyte differentiation was usually complete by day 8. Oil Red O/ haematoxylin staining, x200.

(a) 3T3-L1 preadipocytes demonstrated a fibroblast-like morphology 2 d after seeding.

(b) Day 0: 48 h after cells became 100% confluent, usually 5-6 days after seeding.

(c) Day 8: 3T3-L1 cells had an adipocyte like morphology with much more rounded cytoplasm full of lipid droplets stained red with Oil Red O

(d) Day 8: 3T3-L1 cells which were not stimulated with insulin, IBMX and dexamethasone. There was approximately 1 differentiated cell/ hpf.